Proceedings of the ASME 2010 3rd Joint US-European Fluids Engineering Summer Meeting and 8th International Conference on Nanochannels, Microchannels, and Minichannels
FEDSM-ICNMM2010
August 1-5, 2010, Montreal, Canada

FEDSM-ICNMM2010-30786

Flowfield Analysis in T-Junction Microchannel with Bubble Formations

Srikanth Pidugu
University of Arkansas at Little Rock
Little Rock, AR, USA

Tarek Abdel-Salam
East Carolina University
Greenvillie, NC, USA

Tuba Bayraktar
University of Wisconsin-Platteville
Fox Valley Engineering Program
Menasha, WI, USA

ABSTRACT

Rapid fluid mixing phenomenon in microchannels offers significant advantages in lab-on-chip testing, drug preparations, micro-assay, and micro-combustor applications. Development of new materials for microchannels and advances in micro fabrication techniques continue to aid fluid mixing research that is vital to microfludic applications. Due to the need for low cost and biocompatibility, polymers began to play important role in design of micromixers. Recently, a number of methods and devices are designed to enhance mixing at the microscale [1-3]. A novel idea of introducing bubbles into two mixing streams with three mixing chambers downstream is tested by means of experiments [3]. The interaction among the bubbles in the mixing chamber results in the stretching and folding of the laminar flow interface leading to a rapid chaotic mixing in short period of time. However, the physics of recirculation zones, bubble formation, and bubble fragmentation must be fully understood in order to design efficient micromixers using this technique. The objective of the present work is to numerically study the formation of recirculation zones, bubble formation, and bubble break-up in microchannels. Numerical calculations were performed with finite volume CFD code ANSYS Fluent. Results obtained with structured grids with about 47,000 grid points. Different gas velocities, liquids velocities and inlet angles were used to investigate the flowfield. Results show that the liquid velocity has a major effect on the circulations inside the channel which impact the formation of the gas bubble. Also, at low liquid velocities, the length of the gas slug is affected by the gas velocity.

NOMENCLATURE

t	time
F	force
$\vec{F}$	force vector
$\vec{g}$	gravitational acceleration
$\vec{n}$	unit normal vector
$\vec{v}$	velocity vector
Greek Letter	
α	volume fraction
θ	angle of gas entry
μ	molecular viscosity, also microns
σ	surface tension
ρ	density
Suffixes	
g	gas
l	liquid
curv	curvature
surf	surface

INTRODUCTION

Microfluidic systems have found application in many areas such as lab-on-chip testing, drug preparations, micro-assay, chemical processes, power generation, cooling of electronic devices, aerospace industry, and inkjet printers. Many of these applications require rapid mixing of fluids.

A novel technique to introduce air bubbles into two moving fluids to aid the mixing of fluids in microfluidic devices is experimentally investigated recently by Mao et al. [3]. A number of experimental and computational studies are carried out in recent past to investigate two phase flows in microchannels, commonly known as Taylor flows [4-6]. Theses studies investigated the bubble formation, bubble fragmentation, and influence of surface tension interaction, surface wetting properties, and contact angle. Most commonly included geometric configurations are T-junction microchannels, Y- junction microchannels, cross section microchannels, and co-flowing microchannels [4, 7-10].

Microscopic gas bubbles have numerous engineering applications. Their potential in biomedical applications such as targeted drug delivery, tumor destruction, and as an enhanced gene vector has been recognized [11]. Interestingly, many researchers also studied bubble formation in microchannels as they present obstacles to flow and thereby effecting the performance of microfludic devices [12]. This problem becomes more severe at narrowed sections. Jensen et al. studied the quasi-static motion of large wetting bubbles in microfluidic channels with contractions and provided design rules for minimizing the clogging pressure of microchannel contractions. Many also recognized salutary effects of presence of bubbles in microfludic devices. A nonmechanical, thermocapillary pumping mechanism was developed for moving discrete drops of liquid within micron-scale flow channels by Sammarco and Burns [13]. These drops actually function as chemical micro-rectors. Ganan-Calvo and Gordillo [11] reported efficient mass production of micron size gas bubbles with a perfectly monodisperse and controllable diameter for creating liquid-gas emulsions in food industry and biomedical applications. Guo and Chen [4] indicated that understanding the characteristics of Taylor flow in microchannels is important for the design of thermal control system on spacecraft. Fu et al. [14] used μ-PIV technique and a high-speed digital camera to visualize the bubble formation in a cross-junction microchannel. They observed various bubble shapes (slug, isolate, and satellite bubbles) at different gas/liquid flow rates. They reported that the collapse time of gas stream is mainly affected by the gas-liquid flow rate.

Many computational studies also carried in recent past to understand Taylor Flows [4-6]. Goel and Buwa [15] investigated bubble formation and their rise in circular capillaries numerically using volume of fluid (VOF) technique. Gupta et al. [6] has provided extensive literature on computational studies carried out to investigate Taylor flows. Literature review revealed that number of researchers successfully used VOF technique to simulate two-phase flows.

While considerable amount of research is in progress to understand the bubble formation and fragmentation and influence of various parameters that affect their formation and growth, not much attention is paid on how the bubble formations and recirculation zones can enhance mixing in microfludic devices. In this work, we investigate immiscible gas-liquid two phase flow in a T-junction microchannel. Our focus of study is specifically at the junction where two fluids meet and how bubbles and recirculation zones are formed. The understanding will help our future mixing studies in microfludic devices.

COMPUTATIONAL MODELING

a. Physical Model

In this study, we used a two-dimensional T-junction microchannel utilized in Guo and Chen's work [4]. The inlet dimension is 200 μm. The length of straight (water) and vertical (air) channels is 600 μm. In our study, we also changed the angle of entry (θ) of air into water. The length of straight mixing channel remained same in all cases and measured at 10.8 mm.

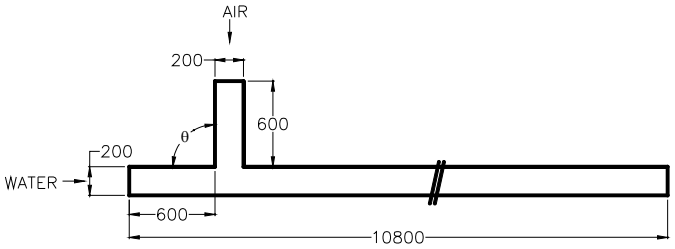

Fig. 1. Physical Model of T-Junction

b. Governing Equations

We used volume of fluid (VOF) method to simulate two-phase flows in microchannels. The VOF method is found to be one of the best methods to simulate complex free surface problems [4-6, 9]. This method allows tracking the interface between the two phases. The details of governing equations are described in detail in many works [4,7] and a brief description will be given here. The governing equations to simulate two-phase flows are continuity, momentum, and equation of continuity for volume fractions.

$$\frac{\partial \rho}{\partial t} + \nabla .\left(\rho \vec{v}\right) = 0 \qquad (1)$$

$$\frac{\partial(\rho\vec{v})}{\partial t}+\nabla.(\rho\vec{v}\vec{v})= -\nabla.p+\nabla.\left[\mu\left(\nabla\vec{v}+\vec{v}^{t}\right)\right]+\rho\vec{g}+\vec{F} \quad (2)$$

$$\frac{\partial\alpha}{\partial t}+\vec{v}.\nabla\alpha=0 \quad (3)$$

As mentioned before, the main purpose of VOF method is tracking of interface between the two phases. Solving of equation for continuity for volume fractions enables to carry out this task.

The surface tension force is treated as a source term in momentum equation and modeled using continuum surface (CSF) model proposed by Brackbill et al. [16]

$$F_{surf}=\sigma\frac{\rho\, r_{curve}\nabla\alpha_g}{\frac{1}{2}\left(\rho_g+\rho_l\right)} \quad (4)$$

The interface curvature r_{curve} in surface tension force is computed as

$$r_{curve}=\nabla.\vec{n} \quad (5)$$

Where $\vec{n}$ denotes the unit normal vector on the interface.

c. Solution Methods and Boundary Conditions

The simulations are carried out using the finite volume CFD code ANSYS Fluent code and two phase flow is modeled using its VOF option. The flow domain is discretized using GAMBIT mesh generation software using quadrilateral cells. The number of cells used in study is based on our understanding of studies using similar physical domains. Guo and Chen [4] reported that cells higher than 9700 gave accurate results. We used 47,190 cells with uniform grid for our computational studies. It may be noted that this grid gave accurate results but could not capture the liquid film at the bubble surface. For future studies, we will use a denser grid with finer mesh near the walls and liquid-gas interface.

Initial studies are carried under steady condition to understand effect of descritization schemes such as QUICK and first order UPWIND scheme and pressure-velocity couplings such as SIMPLE and PISO. After considerable numerical experimentation, we used PISO algorithm for pressure velocity-coupling although it takes slightly more computational time compared to SIMPLE. A second order time stepping scheme is used for time marching of the momentum equation. Descritization of temporal derivations is carried out by means of first order implicit method. PRESTO method is used for the pressure interpolation and geometric construction is used for the interface construction. At the inlet, uniform velocity is specified and pressure outlet boundary condition with zero gage pressure is imposed at the outlet. No slip wall condition is specified at the wall boundary. Value of global Courant number is limited to 0.25 by keeping time step sufficiently small (1×10^{-5} – 1×10^{-6} s). Convergence criterion is set when residuals reached below 0.0001. After steady state achieved, data at different instances of time are analyzed.

Simulations are carried out using water-air combination. The properties are given in the Table 1. A wide range of inlet velocities are specified. Table 2 gives inlet velocities and geometric configurations used in this study. Two angles of entry (90^o and 60^o) for gas are used in this study. Gas and liquid phases are modeled as incompressible fluids with constant viscosity and surface tension. The flow is modeled as laminar flow due to low velocity conditions.

Table 1. Physical Properties of Liquids (300 K and 100 kPa)

Liquid	Density (kg/m3)	Viscosity (mPa-s)	Surface Tension (mN/m)
Water	998	0.95	72
Air	1.185	0.0831	

Table 2. Angle for Gas Entry, Liquid and Gas Velocities

Case	Angle (^{o})	Liquid (Water) Velocity (m/s)	Gas (Air) Velocity (m/s)
A	90	0.038	0.035
B	90	0.028	0.035
C	90	0.09	0.035
D	90	0.1	0.3
E	60	0.028	0.035

RESULTS AND DISCUSSIONS

a. Flowfield analysis

The Figure 2 is presented to show the development of bubble formation for the case of 0.035 m/s air inlet velocity and 0.038 m/s water inlet velocity. The blue color represents the gas phase and the red color represents the liquid phase in Figure 2. The velocity vector plots for the same case are shown in Figure 3. At the time step of 0.03 s, the liquid-phase velocity vectors become inclined towards the left corner of the channel. When the liquid phase is very close to the gas interface, it makes a sharp turn. A circulation of vortex ring in the liquid phase is observed in the lower portion of the channel. The velocity

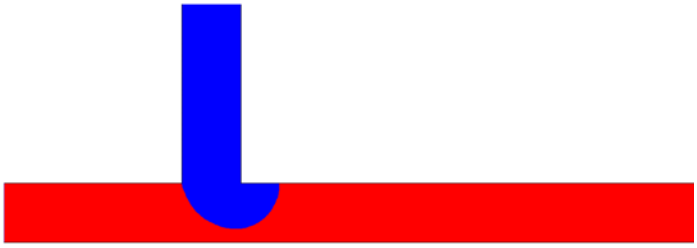

(a) Time step of 0.03 s

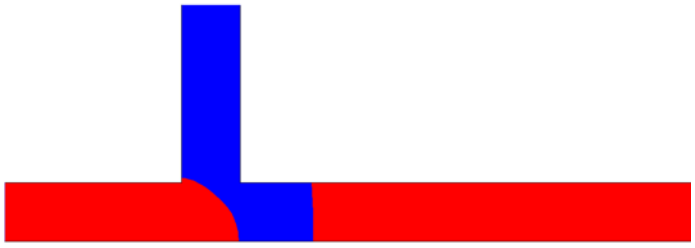

(b) Time step of 0.0325 s

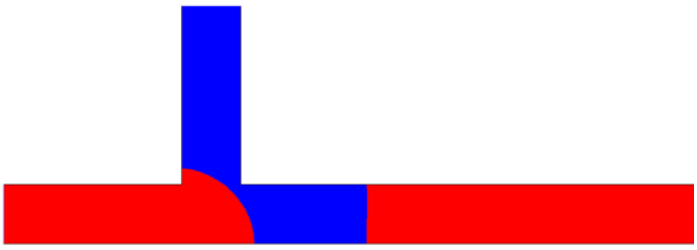

(c) Time step of 0.035 s

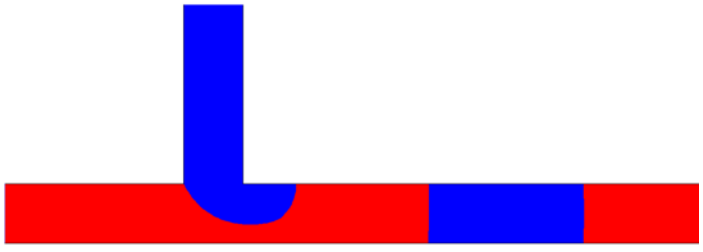

(d) Time step of 0.045 s

Fig. 2. Volume fraction contours for the liquid phase at various time steps for the inlet velocity conditions of V_{gas} = 0.035 m/s and V_{liquid} = 0.038 m/s.

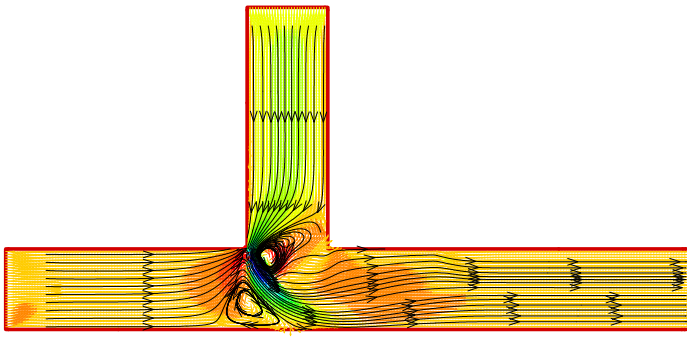

(a) Time step of 0.03 s

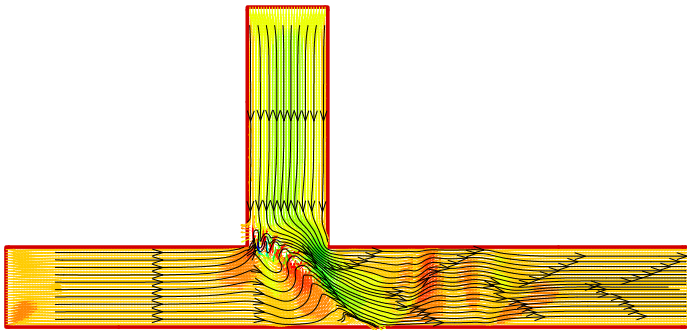

(b) Time step of 0.0325 s

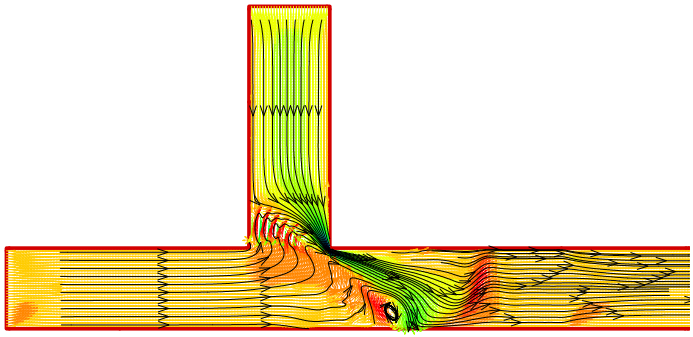

(c) Time step of 0.035 s

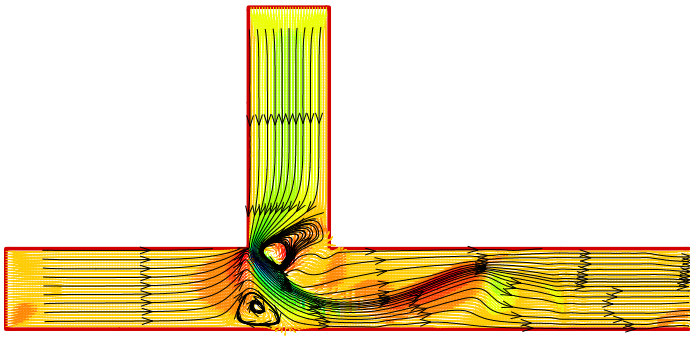

(d) Time step of 0.045 s

Fig. 3. Velocity vector plots at various time steps for the inlet velocity conditions of V_{gas} = 0.035 m/s and V_{liquid} = 0.038 m/s.

vectors of gas phase are also inclined towards the left corner of the channel. The gas phase forms a vortex ring close to the gas-liquid interface. Once the liquid phase passes the gas-liquid interface, it continues to flow in the horizontal direction. At the time step of 0.0325 s, the liquid phase velocity vectors are oriented perpendicular to the gas-liquid interface. It is observed that the liquid phase pushes the gas-liquid interface towards the right corner of the channel. The gas phase fills the horizontal channel separating the liquid flow regions. At the time step of 0.035 s, the main direction of the liquid phase flow around the gas-liquid interface becomes vertical. The interface is pushed very close to the right corner of the channel. Eventually the bubble will break-off at the right corner. A small vortex ring is observed in the air flow towards the bottom wall of the horizontal channel. The liquid phase flow direction on the right side is horizontal. At the time step of 0.045 s, the first bubble detaches and the second bubble starts to form. The vortexes observed in the liquid and gas phases are similar to the time step of 0.03 s during the formation of the first bubble. The liquid phase flow follow the shape of gas- liquid interface around the second emerging bubble.

The bubble formation process is repeated in a similar manner in other time steps, and the slugs of liquid phases separated by gas bubbles are obtained. This is a general characteristic of Taylor flow. We examined cases of various gas and liquid inlet velocity conditions (see Table 2). No collapsing or coalescing bubbles were observed among these cases. Similar observations were made by Guo and Chen [4] and Gupta et al [6].

b. Effect of Liquid Velocity

Figure 4 shows the velocity flow patterns for two liquid inlet velocities (0.028 m/s and 0.09 m/s) at the same time step. The higher liquid inlet velocity condition for the same gas inlet velocity produced larger number of recirculation zones. Comparing the two velocity flowfields, it can be seen that two vortices are created in the mixing zone and one large vortex is created further downstream of the channel when the liquid inlet velocity is equal to 0.09 m/s. However, at lower liquid inlet velocity case, one small vortex is formed in the mixing zone. This is expected since high liquid velocity breaks the gas at a faster rate and aids to create more bubbles of smaller slug length and more mixing. Interestingly, when gas inlet velocity is higher than the liquid inlet velocity, the gas slug length increases (see Fig. 5). Guo and Chen also reported similar trends in their work. [4]

We are further investigating the effect of liquid velocity and we plan on reporting more results in our future publications. We will also intend to report results using non-dimensional numbers such as Capillary number, Reynolds number, and non-dimensional lengths.

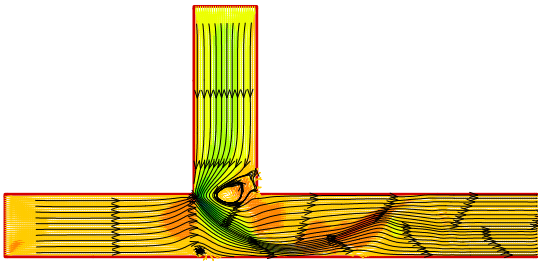

(a) V_{gas} = 0.035 m/s and V_{liquid} = 0.028 m/s

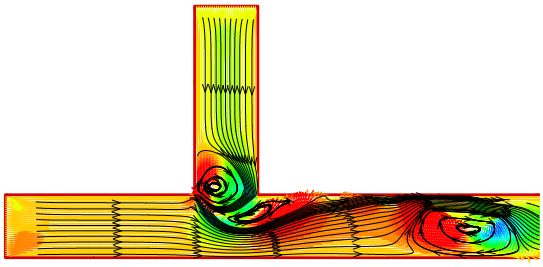

(b) V_{gas} = 0.035 m/s and V_{liquid} = 0.09 m/s

Fig. 4. Velocity vector plots at the same time step for two different inlet liquid velocity conditions.

Fig. 5. Taylor flow at the time step of 0.013 s for the inlet velocity conditions of V_{gas} = 0.3 m/s and V_{liquid} = 0.1 m/s.

c. Effect of Gas Angle Entry

Next, effect of angle of gas entry (θ) is studied on flowfields, specifically on formation of recirculation zones. Figure 6 shows the influence of angle of entry of gas flow on flowfields. When angle of entry is 60^o, there is an increased number of recirculation zones formed at the time step of 0.105 s (Figure 6 (a)) comparing to the angle of entry case of 90^o (Figure 4 (a)). It is prudent to introduce gas at an angle less than 90^o if the objective is to create more circulation zones for the efficient mixing. As many as five vortices are generated at the time step of 0.114 s in the mixing zone and clearly one can see large influence of vortexes in this zone (Figure 6 (b)). The formation of vortices will have significant influence on bubble formation, bubble break-up, number of bubbles formed, and mixing characteristics. Similar trends were also observed in the work published by Bhatelia et al. [17].

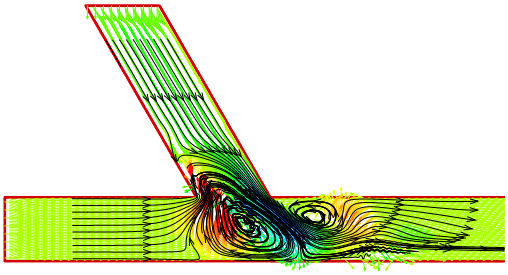

(a) Time step of 0.105 s

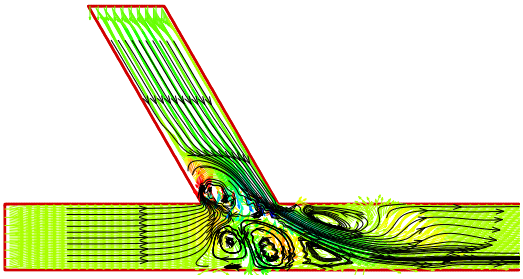

(b) Time step of 0.114 s

Fig. 6. Velocity vector plots for the 60° gas flow angle of entry at two different time steps for the inlet velocity conditions of V_{gas} = 0.035 m/s and V_{liquid} = 0.028 m/s.

d. The Comparison of Numerical Results

Although considerable progress made in understanding the two-phase flows in microchannel, results obtained through experiments are scarce. The following figure is presented to compare the bubble formation in our work with the result from Guo and Chen's work [4]. In Guo and Chen's result the blue color represents the liquid phase and the red color represents the gas phase (Figure 7(a)). It should be noted that in our results the red color represents the liquid phase and the blue color represents the gas phase (Figure 7(b)). Our result compares favorably with Guo and Chen's result. The bubble in our work is not rounded near the wall, probably since we did not simulate the contact angle. This is equivalent to assuming a contact angle of 90°. It is clear that our work captured main flow regimes and other features of two-phase flow in microchannels through computational modeling.

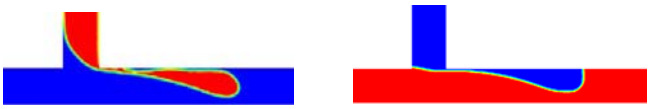

(a) (b)

Fig. 7. Flow regimes near mixing zones (V_{water} = 0.8 m/s and V_{air} = 0.2 m/s) in (a) Guo and Chen's work [4] and (b) our work.

CONCLUSIONS

The characteristics of flowfields in T-junction microchannels were simulated using the finite volume CFD code ANSYS Fluent. The volume of fluid technique was applied successfully to obtain the results in two-phase regime. The flowfields at the mixing zone were examined in detail. The bubble formations, bubble break-up, and creation of recirculation zones were examined. The effect of liquid velocity and angle of gas entry were also studied. For efficient design of micromixers using bubble generation mechanisms, steeper angle of entry (less than 90°) is recommended as it produced a large number of recirculation zones in the mixing region. It was observed that the higher liquid inlet velocity for the same gas inlet velocity condition resulted in more recirculation zones in the microchannel. It was also observed that the high gas inlet velocity and low liquid inlet velocity resulted in longer gas slugs.

REFERENCES

[1] Nguyen, N-T and Wu, Z., 2005, "Micromixers – a review," *Journal of Micromechanics and Microengineering*., 15, pp. R1-R16.

[2] Mansur, E., Mingxing, Y., Yundong, W., and Youyuan, D., 2008, "A State of the Art Review of Mixing in Microfludic Mixers," *Chinese Journal of Chemical Engineering*., 16(4), pp. 502-516.

[3] Mao, X., Juluri, B., Lapsley, M. I., and Huang, T. J., 2008, "Milliseconds Microfluidic Bubble Mixer Using Chaotic Advection," *Proceedings of 2008 ASME International Mechanical Engineering Congress and Exposition*, October 31-November 6, 2008, Boston, Massachusetts, USA.

[4] Guo, F and Chen, B., 2009, "Numerical Study on Taylor Bubble Formation in a Micro-channel T-Junction Using VOF Method," *Microgravity Science and Technology*., 21(Suppl 1): S51–S58.

[5] Rong, S and Chen, B., 2010, "Numerical Simulation of Taylor Bubble Formation in a Micro-channel by MPS Method," *Microgravity Science and Technology*., online publication.

[6] Gupta, R., Fletcher, D. F., and Haynes, B. S., 2009, "On the CFD Modeling of Taylor Flow in Microchannels," *Chemical Engineering Science*., 64, pp. 2941-2950.

[7] Baroud, C. N., and Willaime, H., 2004, "Multiphase Flows in Microfluidics," *C. R. Physique*., 5, pp. 547–555.

[8] Xiong, R., Bai, M., and Chung, J. N., 2007, "Formation of bubbles in a Simple Co-flowing Microchannel," *Journal of Micromechanics and Microengineering.*, 17, pp. 1002-1011.

[9] Akbar, M. K., and Ghiaasiaan, S. M., "Simulation of Taylor Flow in Capillaries Based on the Volume-of-Fluid Technique," *Ind. Eng. Chem. Res.*, 45 (15), pp 5396–5403.

[10] Huh, D., Grotberg, J. B., and Takayama, S., 2009, "Gas-liquid Two-phase Flow Patterns in Rectangular Polymeric Microchannels: Effect of Surface Wetting," *New Journal of Physics*, 11, pp. 1-14

[11] Ganan-Calvo, A., M., and Gordillo, J. M., 2001, "Perfectly Monodisperse Microbubbling by Capillary Flow Focusing," *Physical Review Letters.*, 87(27), pp. 1-4.

[12] Jensen, M. J., Goranovic, G., and Bruus, H., 2004, "The Clogging Pressure of Bubbles in Hydrophilic Microchannel contractions," *Journal of Micromechanics and Microengineering.*, 14, pp. 876-883.

[13] Sammarco, T. S., and Burns, M. A., 1999, "Thermocapillary Pumping of Discrete Drops in Microfabricated Analysis Devices," *AIChE Journal.*, 45(2), pp. 350-366.

[14] Fu, T., Youguang, M., Funfschilling, D., Li, H. Z., 2009, "Bubble Formation and Breakup Mechanism in a Microfluidic Flow-focusing Device," *Chemical Engineering Science*., 64, pp. 2392-2400.

[15] Goel, D., and Buwa, V. V., 2009, "Numerical Simulations of Bubble Formation and Rise in Microchannels," *Ind. Eng. Chem. Res., 48, pp.* 8109–8120.

[16] Brackbill, J.U., Kothe, D.B., Zemach, C., 1992, "A continuum method for modeling surface tension," J. Comput. Phys. 100, 335–354.

[17] Bhatelia, T. J., Utikar, R. P., Pareek, V. K., and Moses O. T., 2009, "Hydrodynamics of Slug Flow in Capillary Microchannels," *University Journal of Engineering and Technology*., 1, pp. 1-9.